

# Toughened Composites Prepared from Castor Oil Based Polyurethane and Soy Dreg by a One-Step Reactive Extrusion Process

Yun Chen,<sup>1,2</sup> Lina Zhang,<sup>1</sup> Rui Deng,<sup>1</sup> Hui Liang<sup>2</sup>

<sup>1</sup>Department of Chemistry, Wuhan University, Wuhan 430072, China

<sup>2</sup>Hubei Key Laboratory of Allergy and Immune-Related Diseases, Medical School, Wuhan University, Wuhan 430072, China

Received 28 January 2005; accepted 17 December 2005

DOI 10.1002/app.24023

Published online in Wiley InterScience (www.interscience.wiley.com).

**ABSTRACT:** A series of water-resistant composites were successfully prepared from a mixture of soy dreg (SD), castor oil, and 2,4-toluene diisocyanate (TDI) by a one-step reactive extrusion (REX) process. The structure and properties of the composites were characterized by Fourier transform infrared spectroscopy, scanning electron microscopy, differential scanning calorimetry, dynamic mechanical analysis, tensile testing, and swelling experiments. The results indicated that the toughness of the composites prepared from castor oil based polyurethane and SD was significantly improved. In this case, TDI played an in situ compatibilization role through the crosslinking reaction of —NCO groups with —NH<sub>2</sub>, —NH—, and —OH groups in SD and castor

oil. With an increase in the molar ratio of —NCO groups of TDI and —OH groups of castor oil, the degree of crosslinking, tensile strength, glass-transition temperature, water resistivity, and solvent resistivity of the composites increased. With an increase in the SD content of the composites, the tensile strength and solvent resistivity of the composites increased because of the reinforcement of the cellulose component in SD. This work provided a simple and effective way of preparing SD-based composites by a REX process.

© 2006 Wiley Periodicals, Inc. *J Appl Polym Sci* 101: 953–960, 2006

**Key words:** composites; crosslinking; reactive extrusion

## INTRODUCTION

Commercially available soy products such as soy protein isolate (SPI), soy flour (SF), and soy protein concentrate (SPC) have been regarded as biodegradable polymer resources with extensive applications in adhesives, plastics, and biomedical fields.<sup>1–5</sup> Soy dreg (SD) is an abundant byproduct from the isolation process of soy protein, which mainly contains cellulose, dietary fiber, and soy protein.<sup>6</sup> Great attention has been paid to research on SPI and SF to make soy-based plastics in recent years,<sup>7–11</sup> whereas the efforts with SD have been too little.<sup>6,12</sup> The difficult processibility results from no effective ways of dissolving or melting SD, and the poor water resistivity of SD is caused by hydrophilic groups in the protein and cellulose molecular chains. Thus, it is most important for the de-

velopment of SD in material fields to enhance its processibility and water resistivity.

Reactive extrusion (REX) is an effective way of modifying polymers. A one-step process is to directly mix compatibilizers containing reactive groups with two or more polymers having incompatibility or bad compatibility.<sup>13</sup> The compatibility of the polymers in this system can be greatly improved because of the obvious in situ compatibilization of the reactive compatibilizers.<sup>13,14</sup> Zhong and Sun<sup>11</sup> reported that 0.5–5 wt % methylene diphenyl diisocyanate plays a role in the enhancement of the compatibility of blends of SPI and polycaprolactone (PCL). The compatibility, tensile strength, and water resistivity of SPI/PCL blends can be improved by the reaction of —NCO groups with the end reactive groups in SPI and PCL in a one-step REX process. Recently, Narayan et al.<sup>15</sup> reported that biodegradable blends could be prepared by a REX process from SPC and polyester with glycerol as a compatibilizer. However, except for the interactions between functional groups of the protein with glycerol under the conditions of a high temperature and a high shearing force, no other chemical reactions happened in that case.

Castor oil (CO), another natural material, has been used to enhance the water resistivity of wood-based tools via coatings on wood baskets, wood basins, and

Correspondence to: L. Zhang. (lnzhang@public.wh.hb.cn).

Contract grant sponsor: National Natural Science Foundation of China; contract grant number: 20474048.

Contract grant sponsor: Key Laboratory of Cellulose and Lignocellulosic Chemistry of the Chinese Academy of Sciences.

TABLE I  
Compositions and Data of DSC and DMTA of the Composite Sheets

Sample	R	$W_{SD}$ %	$W_{TDI}$ %	$W_{CO}$ % <sup>a</sup>	DSC	DMTA	
					$T_g$ (°C)	$T_g$ (°C)	$\tan \delta_{max}$
STC-50-0	2.00	50.0	16.8	33.2	22.4	49.0	0.26
STC-50-1	1.67	50.0	14.8	35.2	4.70	33.3	0.34
STC-50-2	1.33	50.0	12.6	37.4	-3.30	22.2	0.45
STC-50-3	1.00	50.0	10.1	39.9	-24.3	-1.80	0.68
STC-60-0	2.00	60.0	13.4	26.6	14.7	40.0	0.21
STC-60-1	1.67	60.0	11.8	28.2	—	28.2	0.26
STC-60-2	1.33	60.0	10.0	30.0	—	11.8	0.30
STC-60-3	1.00	60.0	8.1	31.9	—	-5.30	0.47
STC-70-0	2.00	70.0	10.1	19.9	9.90	37.8	0.15
STC-70-1	1.67	70.0	8.8	21.2	—	21.1	0.19
STC-70-2	1.33	70.0	7.5	22.5	—	10.9	0.23
STC-70-3	1.00	70.0	6.0	24.0	—	-29.5	0.25

<sup>a</sup> Weight percentage of in the original mixtures.

boats in China for thousands of years.<sup>16</sup> As its contains three reactive —OH groups in each molecule, it is always used to prepare polyurethane (PU). The structure and properties of natural polymer-based PU could be improved with CO as the soft segment of PU.<sup>17</sup> In practice, it is difficult to blend CO with SD because of their incompatibility. However, blending incompatible materials together with diisocyanate through a one-step REX process is an effective way of enhancing their compatibility. In this case, the —NCO groups in diisocyanate may react with —OH groups in CO and other natural polymers to form new PU molecular chains. Therefore, we attempted to prepare water-resistant composites by mixing SD, 2,4-toluene diisocyanate (TDI), and CO together and then extruded and compression-molded the mixture by *in situ* reactions. The effects of the molar ratio (*R*) of —NCO and —OH groups and the content of SD on the structure and properties of the composites were investigated in this work.

## EXPERIMENTAL

### Preparation of the composite sheets

SD, supplied by DuPont Yunmeng Protein Technology Co. (Yunmeng, China), was milled through an 80-mesh sieve and then treated with acetone and vacuum-dried for 24 h at 60°C. The main components of SD were determined to be about 77 wt % cellulose, 12 wt % protein, and 11 wt % polysaccharide.<sup>6</sup> TDI, supplied by Shanghai Chemical Reagent Co. (Shanghai, China), was vacuum-dried at 80°C for 2 h before use. CO (hydroxyl value = 163) from Zhenzhou Chemical Factory (Zhenzhou, China) was vacuum-dried at 100°C for 24 h before use.

A mixture of SD, CO, and TDI was pestled in a mortar for 30 min and then extruded by a single-screw extruder (PolyDrive with Rheomex R252, Thermo-

Haake, Karlsruhe, Germany; diameter = 19.1 mm, length/ diameter = 25 : 1). The screw rotation speed was 12 rpm, and the temperature profile along the extruder barrel was 100, 110, and 120°C (from the feed zone to the exit). The extrusion process was repeated. The blends that exited from the extruder were immediately compression-molded by a hot presser (769YP-24b, Tianjin Science and Technology Co., Tianjin, China). The procedure was as follows: 3 g of the material was placed in a mold and covered with a polished stainless steel plate on both sides. The temperature of the molding was controlled to be 120°C, and the pressure was quickly increased from 0.5 to 20 MPa for 1 min and then retained for 7 min. The mold was cooled to 50°C with a fan at a rate of 10°C/min. The sheet was released from the mold and stored in a desiccator. *R* of —NCO groups from TDI and —OH groups from CO was 2.0, 1.67, 1.33, and 1.0, respectively; the weight percentage of SD ( $W_{SD}$ ) in the blends was 50, 60, and 70%, respectively. By changes in *R* and  $W_{SD}$ , a series of sheets (STC series) based on SD, TDI, and CO were prepared. The codes and compositions of the samples are listed in Table I.

### Characterization

Attenuated total reflection/Fourier transform infrared (ATR-FTIR) spectra of the samples were recorded on a Fourier transform infrared (FTIR) spectrometer (1600, PerkinElmer Co., Wellesley, MA). The samples were taken at random from the flat sheets, and data were collected over 16 scans with a resolution of 4  $\text{cm}^{-1}$  at room temperature. The SD powder was mixed with KBr to laminate it for the FTIR analysis in a range of wave numbers from 4000 to 400  $\text{cm}^{-1}$ .

The morphology was observed on a scanning electron microscope (S-570, Hitachi, Ibaraki, Japan) with 20 kV as the accelerating voltage, and the images were

obtained by a high-resolution imaging treatment system (HLPAS-1000, Tongji Medical College, Huazhong University of Science and Technology, Wuhan, China). The samples were frozen in liquid nitrogen and fractured immediately, and then the cross sections were coated with gold for scanning electron microscopy (SEM) observation.

Differential scanning calorimetry (DSC) was measured on a DSC-204 apparatus (Netzsch Co., Selb, Germany) under a nitrogen atmosphere at a heating rate of 10°C/min from -80 to 200°C. Before the test, the specimens were heated from room temperature to 100°C to remove moisture and then cooled to -80°C with liquid nitrogen.

Dynamic mechanical thermal analysis (DMTA) was carried out on a dynamic mechanical thermal analyzer (DMTA-V, Rheometric Scientific Co., Piscataway, NJ) at a frequency of 1 Hz. The samples were dried in a desiccator containing P<sub>2</sub>O<sub>5</sub> for 3 days before the test. The test temperatures ranged from -100 to 300°C with a heating rate of 5°C/min.

The tensile strength and the elongation at break of the sheets in the dry state ( $\sigma_b$  and  $\varepsilon_b$ , respectively) were tested on a universal testing machine (CMT6503, Shenzhen SANS Test Machine Co., Ltd., Shenzhen, China) according to ISO527-2:1993 with a tensile rate of 50 mm/min. The mean values of  $\sigma_b$  and  $\varepsilon_b$  were obtained from more than three specimens, and the standard deviations were calculated. The sheets were immersed in water at 25°C for 1 h, and then the tensile strength and elongation at break of the sheets in the wet state [ $\sigma_{b(\text{wet})}$  and  $\varepsilon_{b(\text{wet})}$ , respectively] were measured in the same way mentioned previously.

The water absorption ( $W_a$ ) was determined according to ASTM Standard D570-81 with minor modification. The samples were vacuum-dried at 50°C for 24 h. Subsequently, they were cooled in a desiccator for a few minutes, weighed ( $W_0$ ), and submerged in distilled water at 25°C for 26 h. The sheets were taken out, the surface moisture was wiped off with a paper towel, and then the sheets were weighed ( $W_1$ ). After the sheets were removed from water, they were vacuum-dried at 50°C for 24 h and weighed again ( $W_2$ ).  $W_a$  was calculated as follows:

$$W_a = \{[(W_1 - W_0) + (W_0 - W_2)]/W_0\} \times 100\% \quad (1)$$

The percentage of weight loss ( $W_w$ ) of the membranes in water was calculated as follows:

$$W_w = [(W_0 - W_2)/W_0] \times 100\% \quad (2)$$

The swelling procedure of the sheets in toluene was tested according to Favre's method with minor modification.<sup>18</sup> The initial dry weight ( $W_i$ ) of the samples was measured, and then the samples were immersed in a sealed flask containing toluene for 5 days to be

balanced. The swollen samples were taken out, the excess solvent on the samples was quickly wiped off, and the samples were weighed ( $W_s$ ). At last, the samples were vacuum-dried at 50°C for 24 h and weighed again ( $W_d$ ). The swelling ratio ( $S$ ) and the percentage of weight loss of the samples in toluene ( $W_t$ ) were calculated as follows:

$$S = [(W_s - W_d)/W_d] \times 100\% \quad (3)$$

$$W_t = [(W_i - W_d)/W_i] \times 100\% \quad (4)$$

## RESULTS AND DISCUSSION

### Structure and morphology

FTIR spectra of SD powder and ATR-FTIR spectra of the STC-50-0, STC-50-3 and STC-70-0 composite sheets with different  $R$  and  $W_{SD}$  values are shown in Figure 1. No obvious absorption of -NCO groups (at ca. 2272 cm<sup>-1</sup>)<sup>19</sup> in the ATR-FTIR spectra of the resulting composites can be observed; this indicates the absence of free -NCO groups. The absorption of N-H and O-H at about 3374 cm<sup>-1</sup> in SD shifts to a lower wavelength as a result of the reactions between -NH<sub>2</sub>, -NH-, and -OH groups in SD and -NCO groups in TDI; this indicates the N-H stretching occurred with hydrogen bonding.<sup>20</sup> The decrease in the relative intensity at 1651 cm<sup>-1</sup> ( $\nu_{C=O}$ , amide I)<sup>21</sup> in SD and the increase at 1724-1732 cm<sup>-1</sup> ( $\nu_{C=O}$  in urethane linkages) in the composites suggest that new urethane bonds formed in the composites.<sup>22</sup> At the same time, the increase in the relative intensity at about 1530 cm<sup>-1</sup> ( $\delta_{N-H} + \nu_{C=O}$  in urea linkages, amide II) and 1219 cm<sup>-1</sup> ( $\delta_{C-N} + \delta_{N-H}$  in urea linkages, amide III) indicates the formation of new urea bonds in the composites.<sup>22,23</sup> The results from ATR-FTIR show that the -NCO groups in TDI reacted with -NH<sub>2</sub>, -NH-, and -OH groups in SD and CO to form new urea and urethane bonds. In general, -NH<sub>2</sub>, -NH-, and -OH groups compete with one another when they react with -NCO groups, and -NH<sub>2</sub> exhibits higher reactivity than the -OH group. However, under the conditions of a high temperature and shearing force in the extrusion process, the -OH groups in CO also exhibited high reactivity with -NCO groups. Therefore, TDI played an in situ compatibilization role by its reaction with SD and CO simultaneously in the complex system, resulting in an increase in the compatibility of SD and CO and an enhancement of the processibility of the mixtures.

Because there are two -NCO groups in every TDI molecule, three -OH groups in every CO molecule, and many reactive groups such as -NH<sub>2</sub>, -NH-, and -OH in every protein and cellulose molecular chain, the formation of PU crosslinking networks was undoubted in the reaction and compression-molding

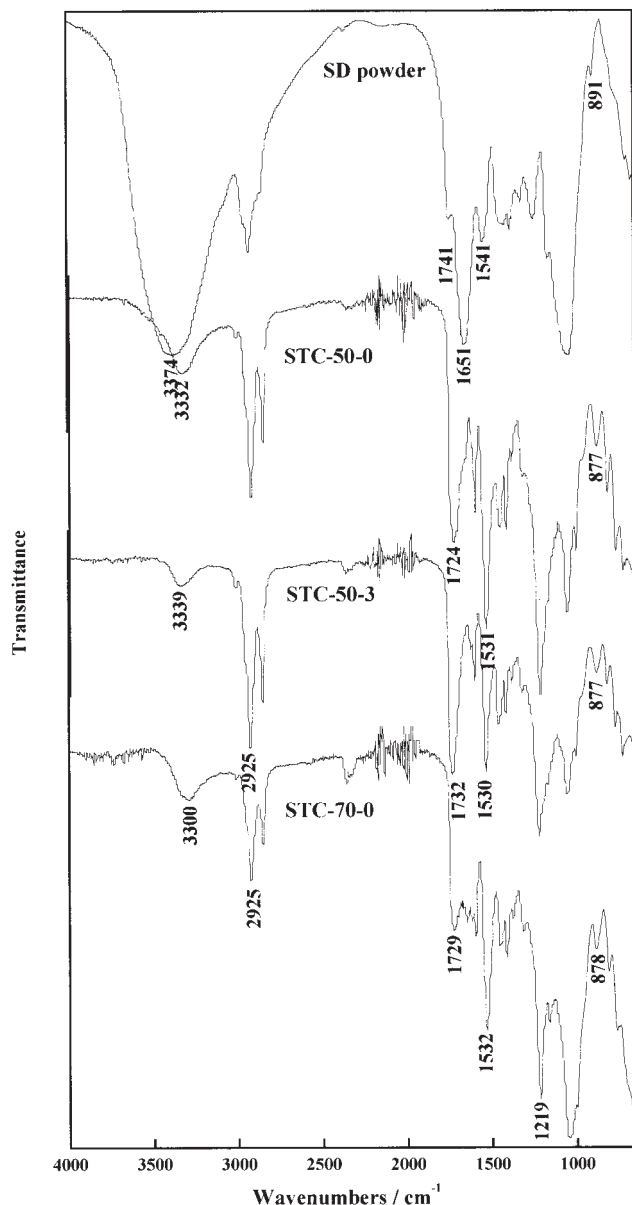


**Figure 1** IR spectra of the SD powder and composites with different  $R$  and  $W_{SD}$  values.

process. In this case, TDI molecules acted as bridges to crosslink CO, soy protein, and cellulose molecules together to form PU networks. The degree of the crosslinking networks increased with an increase in the  $R$  value. Most of the soy protein, CO, and cellulose reacted with TDI during this process. However, the cellulose, protein, and CO, which did not react with TDI, were filled in the networks as fillers. TDI greatly enhanced the compatibility of SD and CO, which were incompatible because of the hydrophilicity of SD and hydrophobicity of CO.

SEM images of cross sections for composite sheets with different  $R$  and  $W_{SD}$  values are shown in Figure 2. Because SD contains several components and more

complex components formed in the heterogeneous reaction and extrusion process, multiphases with different components were observed in the cross sections. From STC-50-0 to STC-60-0 to STC-70-0 in Figure 2, the roughness and phase separation in the cross sections of the sheets with the same  $R$  value (2.0) and different  $W_{SD}$  values (50, 60, and 70 wt %) increased with an increase in  $W_{SD}$ . From STC-50-0 to STC-50-1 to STC-50-2 to STC-50-3, when  $W_{SD}$  (50 wt %) was the same, the roughness in the cross sections of the sheets increased with a decrease in  $R$  from 2.0 to 1.0. This showed that the adhesion and compatibility of the components decreased with an increase in  $W_{SD}$  and a decrease in  $R$ .

### Thermal and mechanical properties

DSC thermograms are shown in Figure 3, and the corresponding data for the composites are listed in Table I. The glass-transition temperature ( $T_g$ ) from  $-24$  to  $22^\circ\text{C}$  has been assigned to  $T_g$  of the PU component in the composites because cellulose and soy protein, the main components in SD, have no obvious glass transitions in this temperature range. For the composites with the same  $W_{SD}$  value (50 wt %),  $T_g$  of the PU component increased from  $-24.3$  to  $22.4^\circ\text{C}$  with an increase in  $R$  from 1 to 2.0 as a result of an increase in the degree of crosslinking with an increase in the TDI content<sup>24</sup> [weight percentage of TDI ( $W_{TDI}$ )] from 10.1 to 16.8 wt %. For the composites with the same  $R$  value (2.0),  $T_g$  decreased from  $22.4$  to  $9.9^\circ\text{C}$  with an increase in  $W_{SD}$  from 50 to 70 wt %. However,  $W_{TDI}$  is not the only factor influencing  $T_g$ . For example,  $T_g$  in the STC-50-3 sheet ( $R = 1.0$ ,  $W_{SD} = 50$  wt %,  $W_{TDI} = 10.0$  wt %,  $T_g = -24.3^\circ\text{C}$ ) is very different from that in STC-70-0 ( $R = 2.0$ ,  $W_{SD} = 70$  wt %,  $W_{TDI} = 10.1$  wt %,  $T_g = 9.9^\circ\text{C}$ ). Therefore, the value of  $R$  also has a great effect on  $T_g$  of the PU component in the composites because of the effect of  $R$  values on the microphase structure of the composites. In this case, SD competes with CO to react with TDI in a mixture of TDI, CO, and SD. Therefore, with an increase in the  $R$  values, SD has more chances than CO to react with TDI, and this results in the formation of more rigid PU chains and more crosslinking domains containing cellulose and protein molecules and in an increase in  $T_g$  of the PU component in the composites.

The dependence of  $\tan \delta$  on the temperature for composites with different  $R$  and  $W_{SD}$  values is shown in Figure 4, and the corresponding data are summarized in Table I. The  $\alpha$  transition in DMTA corresponds to the glass transition of PU. For the composites with the same  $W_{SD}$  value (e.g.,  $W_{SD} = 50$  wt %), with an increase in  $R$  from 1.0 to 2.0,  $T_g$  of the PU component increased from  $-1.8$  to  $49^\circ\text{C}$ , and the height of the  $\tan \delta$  peak decreased from 0.68 to 0.26; this indicated that the increase in the  $R$  value in-

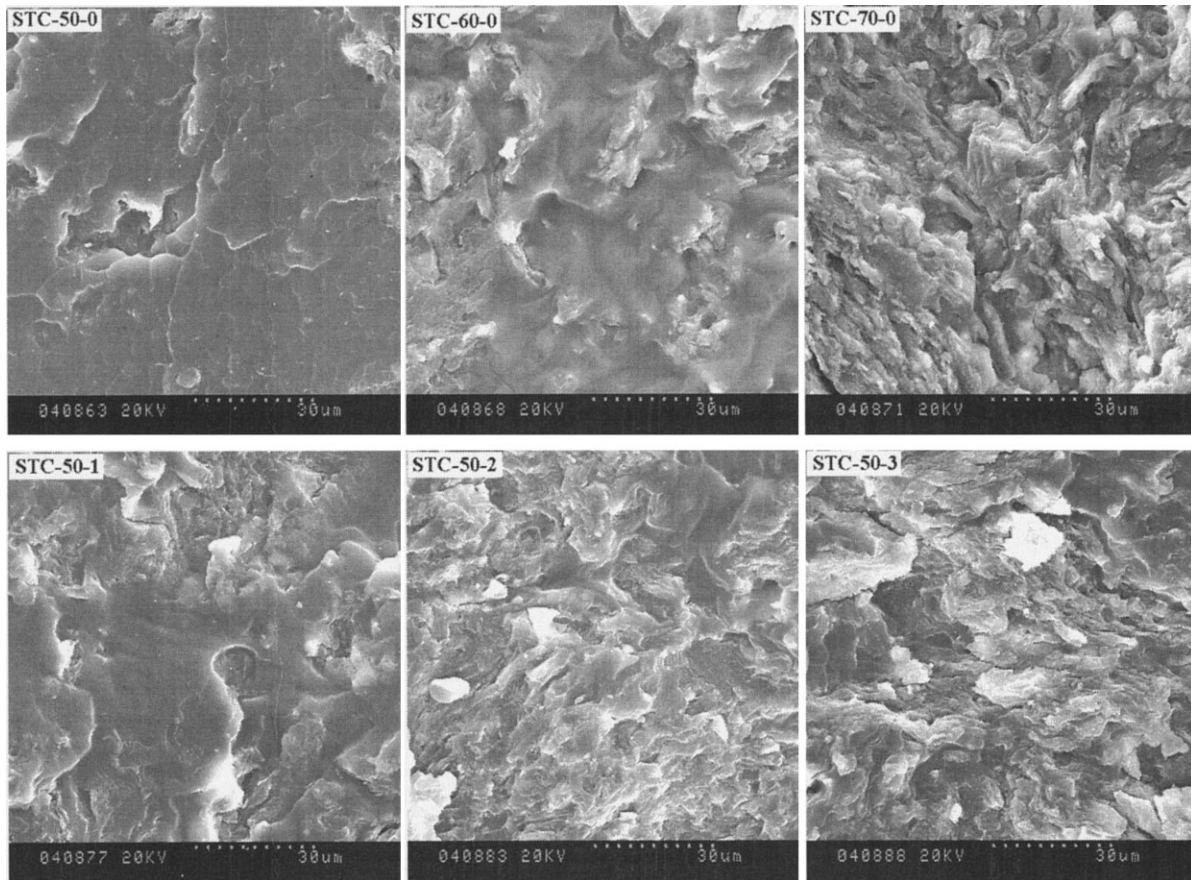


Figure 2 SEM images of cross sections of composite sheets with different  $R$  and  $W_{SD}$  values.

creased the degree of crosslinking and limited the motion of PU molecules. When the  $R$  value was the same (e.g.,  $R = 2.0$ ),  $T_g$  decreased, and the height of the  $\tan \delta$  relaxation peak decreased with an increase in  $W_{SD}$ . Multipieaks occurred in the composite with  $W_{SD} = 70$  wt %, and the height of  $\tan \delta$  and  $T_g$  decreased as

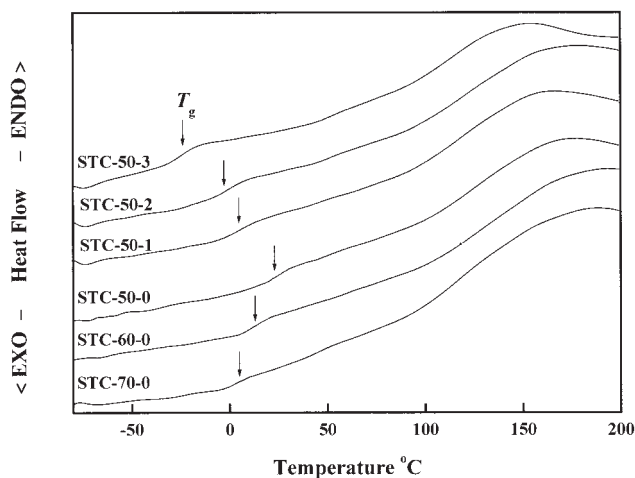
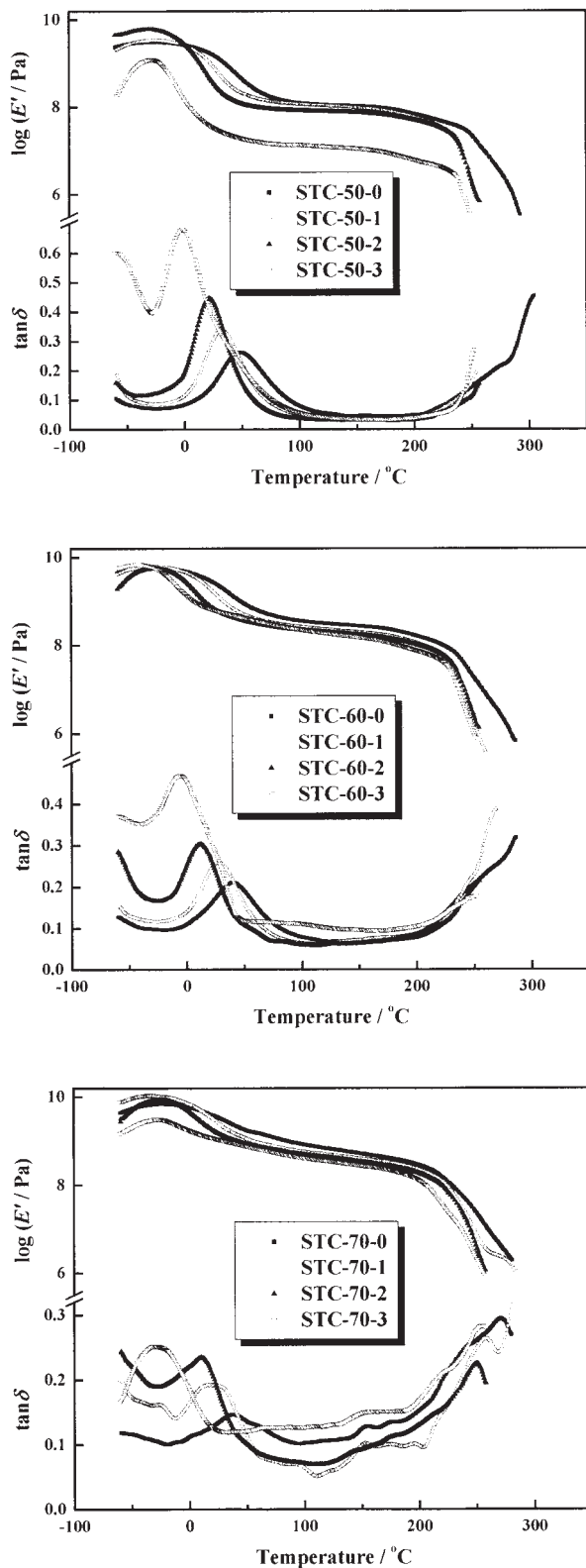


Figure 3 DSC thermograms of composite sheets with different  $R$  and  $W_{SD}$  values.

a result of the decrease in the TDI and CO contents in the composites. In this case, more complex components containing crosslinked PU and uncrosslinked SD coexisted to result in multimolecular motions, and the crosslinking network and compatibility decreased. Therefore, the result from DMTA showed that the composites prepared with higher  $R$  values and lower  $W_{SD}$  values exhibited a higher degree of crosslinking. The  $T_g$  value obtained from DMTA was about 30°C higher than that measured by DSC because of the dynamic nature of the DMTA test.<sup>25</sup> A similar phenomenon was observed in other PU and PU interpenetrating networks modified by natural polymers.<sup>17,26</sup>

Figure 5 shows the effects of the  $R$  value on  $\sigma_b$  and  $\varepsilon_b$  of composite sheets. In comparison with composites prepared from SD with glycerol,<sup>6,12</sup> the composites prepared from TDI, CO, and SD exhibited higher  $\sigma_b$ ,  $\varepsilon_b$ , and toughness because of the introduction of —NCO groups and the formation of PU molecular chains. With an increase in the  $R$  value,  $\sigma_b$  increased rapidly.  $\sigma_b$  of the composite with  $R = 2.0$  and  $W_{SD} = 70$  wt % reached 22.4 MPa. For the composites with the same  $W_{SD}$  value (50 wt %), with an increase in  $R$  from 1.0 to 2.0,  $\sigma_b$  increased from 1.82 to 15.9 MPa, indicating the great effect of the  $R$  value on the tensile



**Figure 4** Dependence of  $\tan \delta$  and the storage modulus ( $\log E'$ ) on the temperature for composite sheets with different  $R$  and  $W_{SD}$  values.

strength. With an increase in the  $R$  value, the degree of crosslinking increased, and this resulted in an increase in the tensile strength of the composite.<sup>27–30</sup> At the

same  $R$ ,  $\sigma_b$  also increased with an increase in  $W_{SD}$  as a result of the reinforcement of the cellulose component in SD. With an increase in  $W_{SD}$ ,  $\epsilon_b$  of the composites increased as a result of the decrease in the crosslinking network. The composite with  $R = 1.33$  and  $W_{SD} = 50\%$  exhibited the highest  $\epsilon_b$  value. It has been reported that PU-based composite materials prepared by a one-step REX exhibit higher  $\sigma_b$  values than those by a two-step REX when the compositions are the same.<sup>28</sup> In comparison with the two-step REX in our work with the same  $R$  and  $W_{SD}$  values, the advantages of the one-step REX are as follows: the processing is shorter; the tensile strength, water resistivity, and solvent resistivity are higher on the whole; and the TDI content in composites with similar properties is lower.

$\sigma_{b(wet)}$  and  $\epsilon_{b(wet)}$  of the composite sheets are shown in Figure 6. The  $\sigma_{b(wet)}$  values of the composites are lower than the  $\sigma_b$  values shown in Figure 5. However, the  $\epsilon_{b(wet)}$  values are higher than the  $\epsilon_b$  values of the sheets as a result of the plasticization of water to the soy protein component.

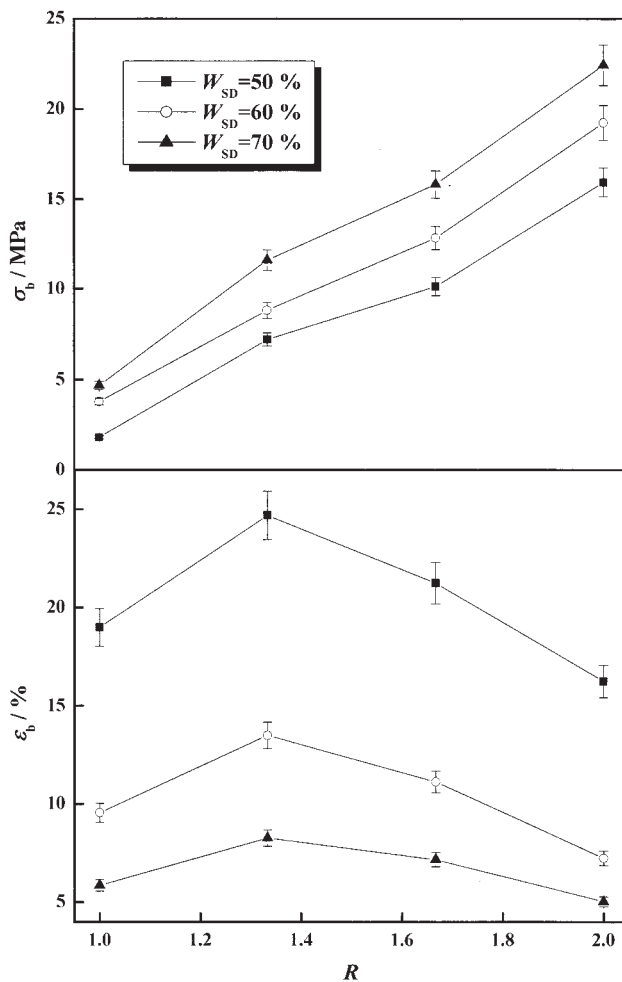


**Figure 5** Effects of  $R$  on  $\sigma_b$  and  $\epsilon_b$  of composite sheets.

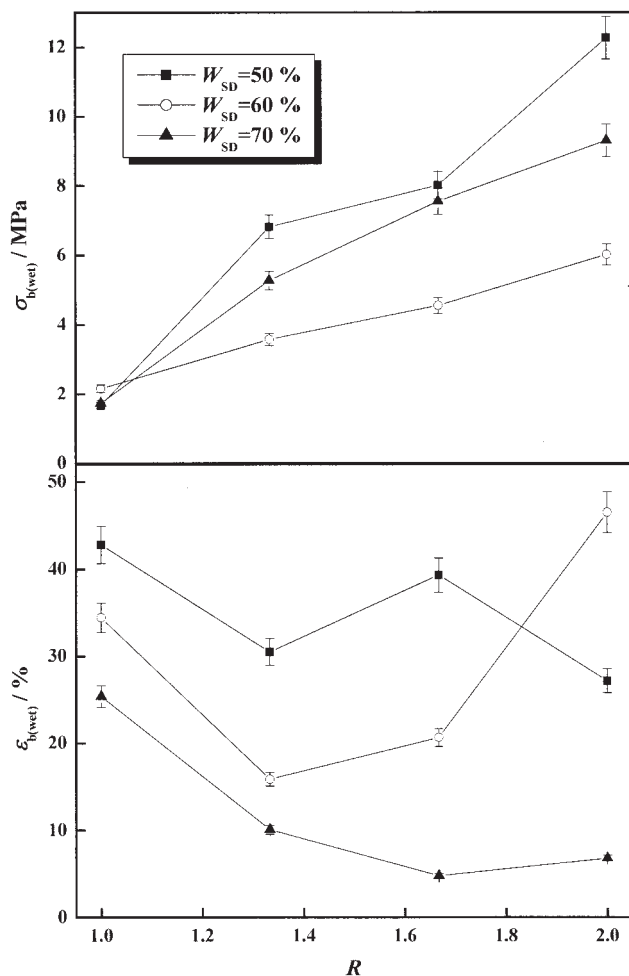


Figure 6 Effects of  $R$  on  $\sigma_{b(wet)}$  and  $\epsilon_{b(wet)}$  of composite sheets.

### Water and solvent resistivity

$W_a$  and  $W_w$  of the composites dipped in water are shown in Figure 7. The results indicated that the  $W_a$  values ranged from 32 to 68%. The water resistivity of the composites increased with an increase in  $R$  as a result of an increase in the degree of crosslinking.  $W_w$  of the composites dipped into water for 24 h was less than 4%, indicating that the formation of a PU crosslinking network greatly inhibited the SD component in the composites from dissolving into water. With an increase in the  $R$  value, both  $W_a$  and  $W_w$  of the composites decreased, and this resulted in an increase in the water resistivity. Interestingly, the composite with  $R = 1.33$  exhibited the highest elongation at break and water resistivity. This suggested that the important factors affecting the physical properties of the composites included not only the degree of crosslinking, decided by  $R$ , and  $W_{SD}$ , but also a certain  $R$  value of the  $-\text{NCO}$  groups reacted with SD and the  $-\text{NCO}$  groups reacted with CO.

$S$  and  $W_t$  of the composites in toluene are shown in Figure 8. With an increase in the  $R$  value, the  $S$  value

decreased as a result of the increase in the degree of crosslinking. With an increase in  $W_{SD}$ , the  $S$  value also decreased, and this was attributed to the oleophobic SD crosslinking with CO in the composites. Therefore, the sheets exhibited a certain toluene resistivity. Their weight loss mainly came from the unreacted CO and linear PU molecules.  $W_t$  of the composites with  $R = 1.0$  ranged from 4 to 6.5%, and this indicated that a small amount of CO did not react with TDI and was easily dissolved in toluene. However,  $W_t$  of the composites with  $R > 1.33$  was less than 1%, and this suggested that most CO reacted with TDI to form a crosslinking network. This indicated that the  $-\text{OH}$  groups in CO easily reacted with  $-\text{NCO}$  groups in TDI at a certain temperature and pressure. In a word, TDI played an in situ compatibilization role by the crosslinking reaction of  $-\text{NCO}$  groups with  $-\text{NH}_2$ ,  $-\text{NH}-$ , and  $-\text{OH}$  groups in SD and CO during the one-step REX process, which greatly contributed to the improvement of the processibility, mechanical properties, water resistivity, and solvent resistivity of the composites.

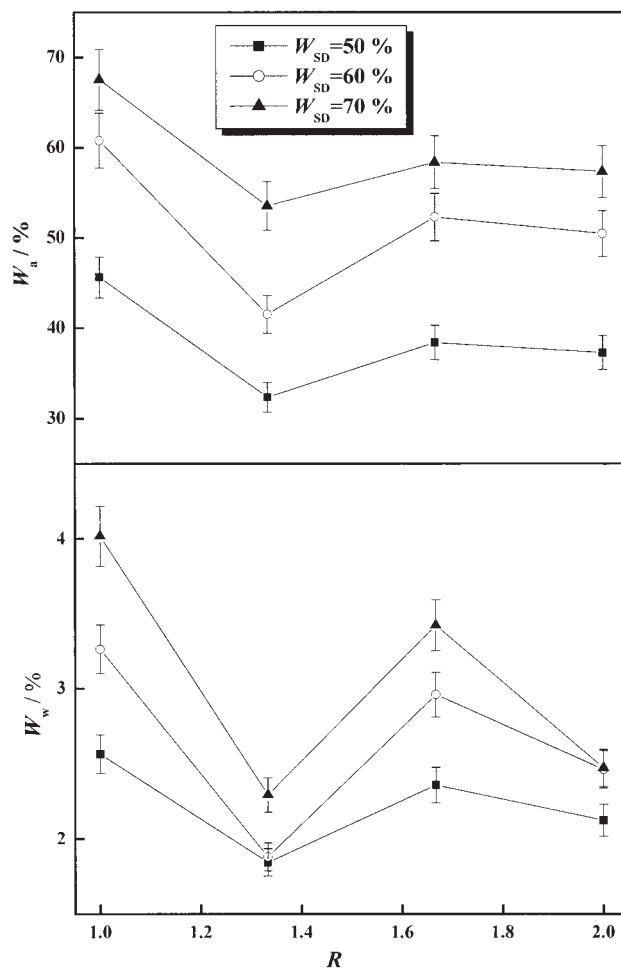
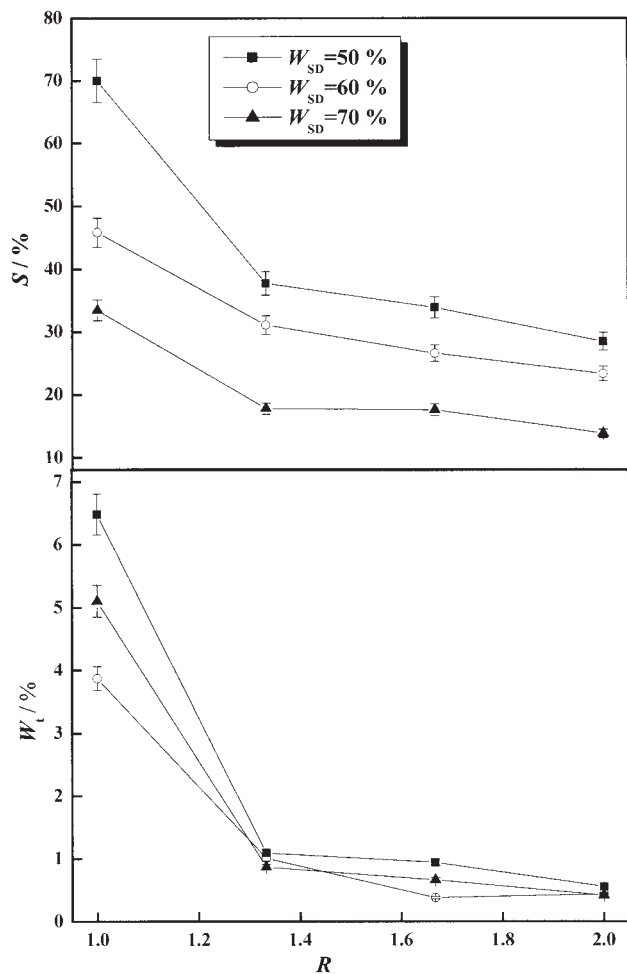


Figure 7 Effects of  $R$  on  $W_a$  and  $W_w$  of composite sheets with different  $W_{SD}$  values.



**Figure 8** Effects of  $R$  on  $S$  and  $W_t$  in toluene of composites with different  $W_{SD}$  values.

### CONCLUSIONS

A series of composite sheets based on SD and CO were successfully prepared by a one-step REX and compression-molding process without the addition of a plasticizer. The composites exhibited good mechanical properties, water resistivity, and solvent resistivity as a result of the formation of a crosslinking structure. TDI, as the reactive compatibilizer, played an important role in in situ compatibilization during the REX process, leading to an improvement of the compatibility between SD and CO. The  $R$  value of —NCO groups from TDI and —OH groups from CO and  $W_{SD}$  in the original mixture had great effects on the structure and properties. With an increase in  $R$ , the degree of

crosslinking increased, and this improved the processibility,  $T_g$ , tensile strength, water resistivity, and solvent resistivity of the composites. With an increase in  $W_{SD}$ , the tensile strength of the sheets increased, whereas  $S$  of the composites decreased. In comparison with the two-step process, the one-step REX process provided shorter processing, better properties, and a more environmentally friendly formula and process.

### References

- Swain, S.; Biswal, S. M.; Nanda, P. K.; Nayak, P. L. *J Polym Environ* 2004, 12, 35.
- Graiver, D.; Waikul, L. H.; Berger, C.; Narayan, R. *J Appl Polym Sci* 2004, 92, 3231.
- Rangavajhyala, N.; Ghorpade, V.; Hanna, M. *J Agric Food Chem* 1997, 45, 4204.
- Kumar, R.; Choudhary, V.; Mishra, S.; Varma, I. K.; Mattiason, B. *Ind Crops Prod* 2002, 16, 155.
- Swain, S.; Biswal, S. M.; Nanda, P. K.; Nayak, P. L. *J Polym Environ* 2004, 12, 35.
- Zhang, L.; Chen, P.; Huang, J. *J Appl Polym Sci* 2003, 88, 422.
- Paetau, I.; Chen, C. Z.; Jane, J. *Ind Eng Chem Res* 1994, 33, 1821.
- Paetau, I.; Chen, C. Z.; Jane, J. *J Environ Polym Degrad* 1994, 2, 211.
- Sue, H. J.; Wang, S.; Jane, J. *Polymer* 1997, 38, 5035.
- Zhang, J.; Mungara, P.; Jane, J. *Polymer* 2001, 42, 2569.
- Zhong, Z. K.; Sun, X. S. *Polymer* 2001, 42, 6961.
- Chen, Y.; Zhang, L.; Ye, C.; Du, L. *J Appl Polym Sci* 2003, 90, 3790.
- Sun, Y.; Hu, G.; Lambla, M.; Kotlar, H. K. *Polymer* 1996, 37, 4119.
- Ignatov, V. N.; Carraro, C.; Tartari, V.; Pippa, R.; Scapin, M.; Pilati, F.; Berti, C.; Toselli, M.; Fiorini, M. *Polymer* 1997, 38, 195.
- Graiver, D.; Waikul, L. H.; Berger, C.; Narayan, R. *J Appl Polym Sci* 2004, 92, 3231.
- Gong, P.; Zhang, L. *Ind Eng Chem Res* 1998, 37, 2681.
- Gao, S.; Zhang, L. *Macromolecules* 2001, 34, 2202.
- Favre, E. *Eur Polym J* 1996, 32, 1183.
- Li, S.; Vatanparast, R.; Lemmetyinen, H. *Polymer* 2000, 41, 5571.
- Monteiro, E. E. C.; Fonseca, J. L. C. *Polym Test* 1999, 18, 281.
- Kurimoto, Y.; Takeda, M.; Yamauchi, S.; Doi, S.; Tamura, Y. *Bioresour Technol* 2000, 74, 151.
- Wu, Y.; Sellitti, C.; Anderson, J. M.; Hiltner, A.; Londoan, G. A.; Payet, C. R. *J Appl Polym Sci* 1992, 46, 201.
- Spathis, G.; Niaounakis, M.; Kontou, E.; Apekis, L.; Pissis, P.; Christodoulides, C. *J Appl Polym Sci* 1994, 54, 831.
- Desai, S.; Thakore, I. M.; Sarawade, B. D.; Devi, S. *Eur Polym J* 2000, 36, 711.
- Martin, D. J.; Meijs, G. F.; Renwick, G. M.; Gunatillake, P. A.; McCarthy, S. J. *J Appl Polym Sci* 1996, 60, 557.
- Huang, J.; Zhang, L. *Polymer* 2002, 43, 2287.
- Petrović, Z. S.; Zhang, W.; Zlatanic, A.; Lava, C. C.; Ilavsky, M. *J Polym Environ* 2002, 10, 5.
- Huang, S. L.; Lai, J. Y. *Eur Polym J* 1997, 33, 1563.
- Hsu, J. M.; Yang, D. L.; Huang, S. K. *Thermochim Acta* 1999, 333, 73.
- Sekkar, V.; Bhagawan, S. S.; Prabhakaran, N.; Rao, M. R.; Ninan, K. N. *Polymer* 2000, 41, 6773.